

# Sensitivity of SnO<sub>2</sub> non-ohmic behavior to the sintering process and to the addition of La<sub>2</sub>O<sub>3</sub>

M.M. Oliveira<sup>a</sup>, P.R. Bueno<sup>a,\*</sup>, M.R. Cassia-Santos<sup>a</sup>, E. Longo<sup>a</sup>, J.A. Varela<sup>b</sup>

<sup>a</sup>*CMDMC-LIEC, Centro Multidisciplinar para Desenvolvimento de Materiais Cerâmicos-Laboratório Interdisciplinar de Eletroquímica e Cerâmica, Departamento de Química,*

*UFSCar, PO Box 676, 13560, São Carlos, SP, Brazil*

<sup>b</sup>*Instituto de Química, UNESP, PO Box 355, CEP.: 14801-970. Araraquara, SP, Brazil*

Received 20 July 2000; received in revised form 25 November 2000; accepted 9 December 2000

## Abstract

The work reported here consisted of a study of the sensitivity of the nonlinear electrical properties of dense SnO<sub>2</sub>-CoO ceramic systems to low concentrations of La<sub>2</sub>O<sub>3</sub>, sintering temperature and cooling rates. The nonlinear electrical properties of these systems were found to increase with decreasing cooling rates, a behavior attributed to the CoO solid state reactions at temperatures below 1000°C. Post-annealing treatment in N<sub>2</sub>-rich atmospheres strongly decreases the non-ohmic behavior of SnO<sub>2</sub>-CoO ceramic systems. However, this behavior may be restored through thermal treatment in an O<sub>2</sub>-rich atmosphere. © 2001 Elsevier Science Ltd. All rights reserved.

*Keywords:* Electrical properties; La<sub>2</sub>O<sub>3</sub>; Sintering; SnO<sub>2</sub>; Varistors

## 1. Introduction

Tin dioxide is an *n* type semiconductor whose tetragonal crystalline structure is similar to the rutile one.<sup>1</sup> Pianaro et al.<sup>2</sup> were the first to present a SnO<sub>2</sub>-based system as the main candidate to substitute multi-component ZnO varistors. In this varistor system, the addition of CoO to SnO<sub>2</sub> leads to high densification,<sup>2–3</sup> which makes it possible to define the varistors' behavior. A high nonlinearity coefficient of  $\alpha = 41$  is obtained in the SnO<sub>2</sub>-CoO-Nb<sub>2</sub>O<sub>5</sub> (1.0 mol% of CoO and 0.05 mol% of Nb<sub>2</sub>O<sub>5</sub>) system when 0.05 mol% of Cr<sub>2</sub>O<sub>3</sub> is added. The major advantage of this system lies in its apparently simple microstructure and its high electrical stability.<sup>4</sup>

The influence of atmosphere treatment on  $\alpha$  and  $E_b$  values in the SnO<sub>2</sub>-CoO-Ta<sub>2</sub>O<sub>5</sub>-Cr<sub>2</sub>O<sub>3</sub> was recently verified.<sup>6</sup> The degradation of the voltage barrier of SnO<sub>2</sub>-based varistors, when heat treated in nitrogen, and the subsequent restoration of this voltage barrier by heat treating in an oxygen atmosphere, suggests that the

chemical origin of the interface states may be chemisorption of oxygen on the grain surfaces.

Bueno et al.<sup>5</sup> recently characterized the nature of the potential barrier in SnO<sub>2</sub>-based varistor systems using a complex plane analysis technique and a Mott-Schottky approach to demonstrate that these systems have a Schottky-type nature (electrostatic potential barrier), i.e. the same nature frequently reported on for the traditional ZnO based varistor system. These findings are important inasmuch as they begin to provide evidence that the nature of nonlinearity in SnO<sub>2</sub>-CoO-based varistor systems may be the same as that observed in ZnO-Bi<sub>2</sub>O<sub>3</sub>-based varistor systems and is related to a Schottky-type barrier at the grain boundary.

The goal of the present work is to investigate the effect of La<sub>2</sub>O<sub>3</sub> and the sintering process on the electrical properties of the SnO<sub>2</sub>-CoO-Nb<sub>2</sub>O<sub>5</sub> varistor system.

## 2. Experimental procedure

The powder was prepared using the ball milling process in an alcohol media. The oxides used were SnO<sub>2</sub> (Cesbra), CoO (Riedel), Nb<sub>2</sub>O<sub>5</sub> (CBMM) and La<sub>2</sub>O<sub>3</sub> (Aldrich). The composition of the molar systems was

\* Corresponding author.

E-mail address: paulo@iris.ufscar.br (P.R. Bueno).

98.95% SnO<sub>2</sub> + 1.0% CoO + 0.035% Nb<sub>2</sub>O<sub>5</sub> + X% La<sub>2</sub>O<sub>3</sub> (SCNLa), with X equal to 0.05, 0.10, 0.15 and 0.30%. Our chemical analysis of SnO<sub>2</sub> indicated that the main impurities were Pb (<0.01%), Fe (<0.01%), Ge (<0.005%) and Cu (<0.005%), all in mol%.

The powder was pressed into pellets (11.0×1.3 mm) by uniaxial pressing (20 MPa), followed by isostatic pressing at 210 MPa. The pellets were sintered at 1250°C for 2 h, at cooling rates of 10, 5 and 2°C min<sup>-1</sup> and 1300°C for 2 h, at a cooling rate of 2°C min<sup>-1</sup> down to room temperature. Mean grain size was determined by analyzing the SEM micrographs (Zeiss DSM 940A) using the PGT software (ASTM-E112 norm). To take the electrical measurements, silver contacts were deposited on the samples' surfaces, after which the pellets were heat-treated at 400°C for 1 h.

The tetragonal structure of SnO<sub>2</sub> (rutile structure) was confirmed as the single phase by X-ray diffraction (obtained with a Siemens diffractometer, model D-5000, CuK<sub>α</sub> radiation) on the mixed powder.

Current–voltage (*I*–*V*) measurements were taken using a high voltage measure unit (Keithley Model 237). The nonlinear coefficient  $\alpha$  was obtained by linear regression of points on a logarithmic scale of around 1 mA cm<sup>-2</sup> and the breakdown electric field (*E*<sub>b</sub>) was obtained at this current density.

The samples were subjected to treatments in O<sub>2</sub> (under a flux of 10 l/min) and in N<sub>2</sub> (under flux of 10 l/min) atmospheres at 900°C for 30 min. The electrical behavior was checked throughout the above mentioned procedures and after each thermal and atmosphere treatment.

### 3. Results and discussion

The XRD patterns of the compositions studied are shown in Fig. 1. As can be seen, the XRD patterns

indicate a single phase in all the systems. Table 1 presents the relative density of the SCNLa system sintered at 1250 and 1300°C, using a 2°C min cooling rate. The relative density of the systems increased as the sintering temperature increased. Figs. 2 and 3 show the SEM micrographs of compositions sintered at 1250 and 1300°C, using cooling rates of 2°C min<sup>-1</sup>. In agreement with the density values shown in Table 1, it was found that the system's porosity increased with the La<sub>2</sub>O<sub>3</sub> mol% concentration, suggesting that La<sub>2</sub>O<sub>3</sub> acted in the grain boundary region, impairing mass transport during sintering.

Table 2 presents mean grain sizes and breakdown voltage per grain for SCNLa systems. As can be seen, the slower the cooling rate the larger the mean grain size (10°C min<sup>-1</sup> > 5°C min<sup>-1</sup> > 2°C min<sup>-1</sup>). The breakdown voltage per grain is, on average, lower when a cooling rate of 10°C min<sup>-1</sup> is used.

Table 3 shows the  $\alpha$  and *E*<sub>b</sub> values for the systems sintered at 1250°C for 2 h at different cooling rates and 1300°C for 2 h, with a 2°C min<sup>-1</sup> cooling rate. The  $\alpha$  and *E*<sub>b</sub> values are, on average, the same for 2 and 5°C min<sup>-1</sup> cooling rates. However, these values are lower for cooling rates of 10°C min<sup>-1</sup>. Fig. 4 shows the influence of La<sub>2</sub>O<sub>3</sub> concentrations and the sintering process on the *I*–*V* behavior in the SnO<sub>2</sub>–CoO based systems studied.

Table 1  
Relative densities for SCNLa systems sintered at 1250 and 1300°C with a cooling rate of 2°C min<sup>-1</sup>

La <sub>2</sub> O <sub>3</sub> mol%	Sintering temperature	
	1250°C	1300°C
0.05	91.6	97.3
0.10	83.2	94.5
0.15	81.1	95.8
0.30	80.0	94.2

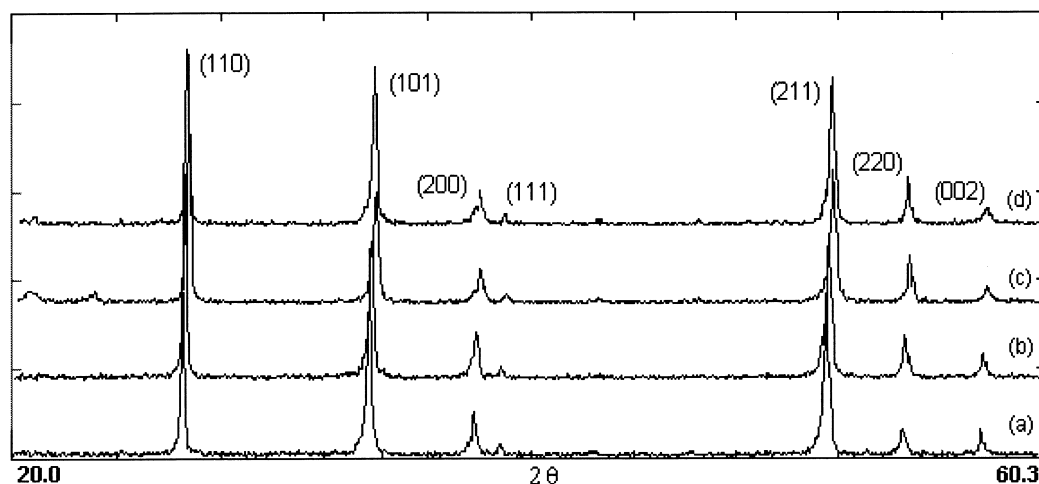


Fig. 1. XRD patterns of SCNLa systems sintered at 1250°C with a cooling rate of 2°C min<sup>-1</sup>: (a) 0.05 mol% of La<sub>2</sub>O<sub>3</sub>; (b) 0.10 mol% of La<sub>2</sub>O<sub>3</sub>; (c) 0.15 mol% of La<sub>2</sub>O<sub>3</sub>; (d) 0.30 mol% of La<sub>2</sub>O<sub>3</sub>.

The cooling rate during processing can increase these values, as previously shown by Leite et al.<sup>6,7</sup> Lowering the cooling rate can cause the  $\alpha$  values to increase from 8 to 24.<sup>6</sup> The increased  $\alpha$  values with slow cooling rates

can be ascribed to the oxidizing effect of CoO during heating to 600°C, followed by reduced effects at temperatures above 1000°C. Eqs. (1)–(3) represent CoO oxidation and reduction:

Table 2

Mean grain size, standard deviation ( $\sigma^{1/2}$ ) and breakdown voltage per grain of SCNLa systems sintering at 1250°C

La <sub>2</sub> O <sub>3</sub> mol%	Cooling rate											
	10°C min <sup>-1</sup>				5°C min <sup>-1</sup>				2°C min <sup>-1</sup>			
	0.05	0.10	0.15	0.30	0.05	0.10	0.15	0.30	0.05	0.10	0.05	0.30
$\bar{d}$ (μm)	5.5	7.6	7.0	4.1	2.3	2.5	2.1	1.6	2.5	2.2	2.0	1.6
$\sigma^{1/2}$	3.5	5.5	6.0	2.1	1.1	1.0	1.0	0.8	1.2	1.1	1.0	0.8
$v_b$ (V/barrier)	0.7	0.8	0.5	1.0	1.7	1.7	2.0	2.0	1.8	1.5	1.0	1.8

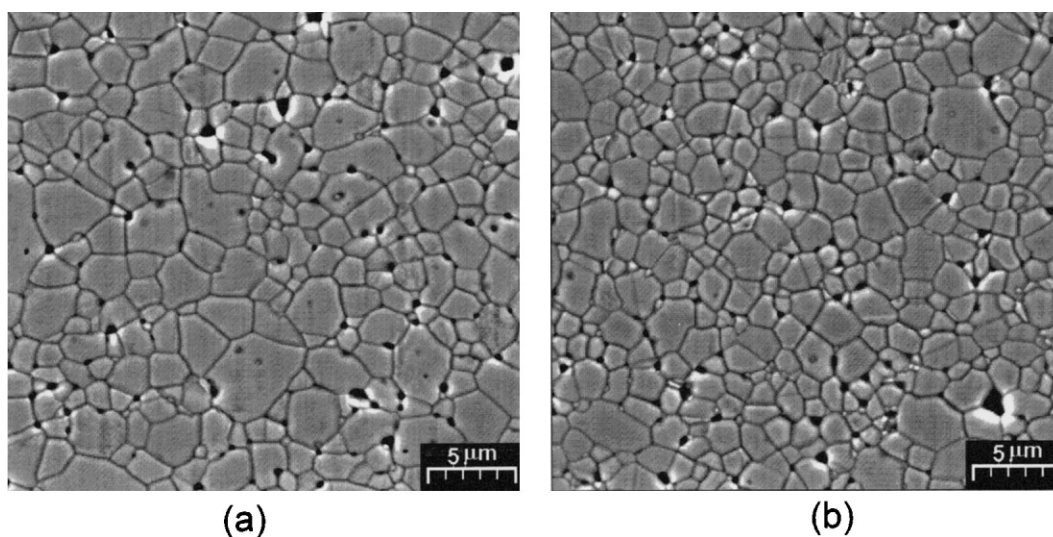


Fig. 2. SEM micrographs of compositions sintered at 1250°C using a cooling rate of 2°C min<sup>-1</sup>: (a) SCNLa with 0.15 mol% of La<sub>2</sub>O<sub>3</sub>; (b) SCNLa with 0.30 mol% of La<sub>2</sub>O<sub>3</sub>.

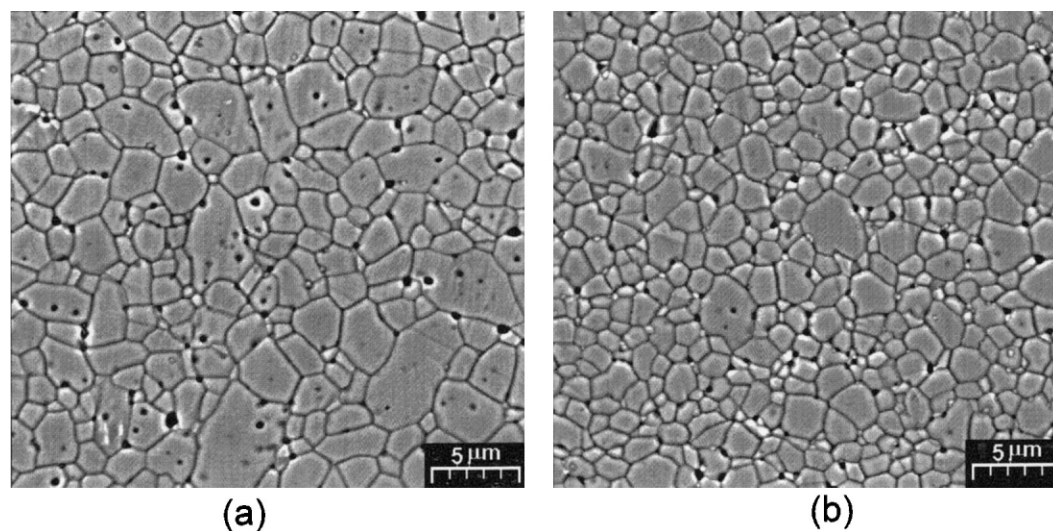
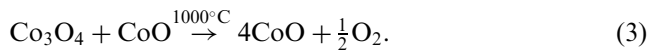
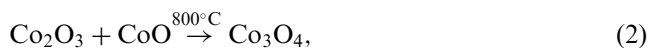


Fig. 3. SEM micrographs of compositions sintered at 1300°C with a cooling rate of 2°C min<sup>-1</sup>: (a) SCNLa with 0.15 mol% of La<sub>2</sub>O<sub>3</sub>; (b) SCNLa with 0.30 mol% of La<sub>2</sub>O<sub>3</sub>.



Cobalt oxide can, thus, affect the trapping state at the grain boundary and modify the potential barrier, according to the cooling rate employed. As Co atoms are precipitated at the grain boundary,<sup>8</sup> depending on the cooling rate, this precipitate may become richer in oxygen through the oxidation of the Co atom (CoO to Co<sub>2</sub>O<sub>3</sub>, for example) below 1000°C, thereby affecting the trapping state in the grain boundary region and, hence, the nonlinear behavior of SnO<sub>2</sub>-based varistors.

Table 3

$\alpha$  And  $E_b$  values for the systems sintered at 1250°C for 2 h using different cooling rates and at 1300°C for 2 h with a cooling rate of 2°C min

La <sub>2</sub> O <sub>3</sub> mol%	ST <sup>a</sup> 1250°C		ST 1250°C		ST 1250°C		ST 1300°C	
	CR <sup>b</sup> 10°C min <sup>-1</sup>		CR 5°C min <sup>-1</sup>		CR 2°C min <sup>-1</sup>		CR 2°C min <sup>-1</sup>	
	$\alpha$	$E_b/V \text{ cm}^{-1}$	$\alpha$	$E_b/V \text{ cm}^{-1}$	$\alpha$	$E_b/V \text{ cm}^{-1}$	$\alpha$	$E_b/V \text{ cm}^{-1}$
0.05	9	1375	22	7426	23	7354	17	4121
0.10	10	1032	21	5957	24	6697	16	2997
0.15	10	677	25	9623	24	5022	19	3637
0.30	13	2400	46	12432	44	11083	17	3999

<sup>a</sup> ST, sintering temperature.

<sup>b</sup> CR, cooling rate.

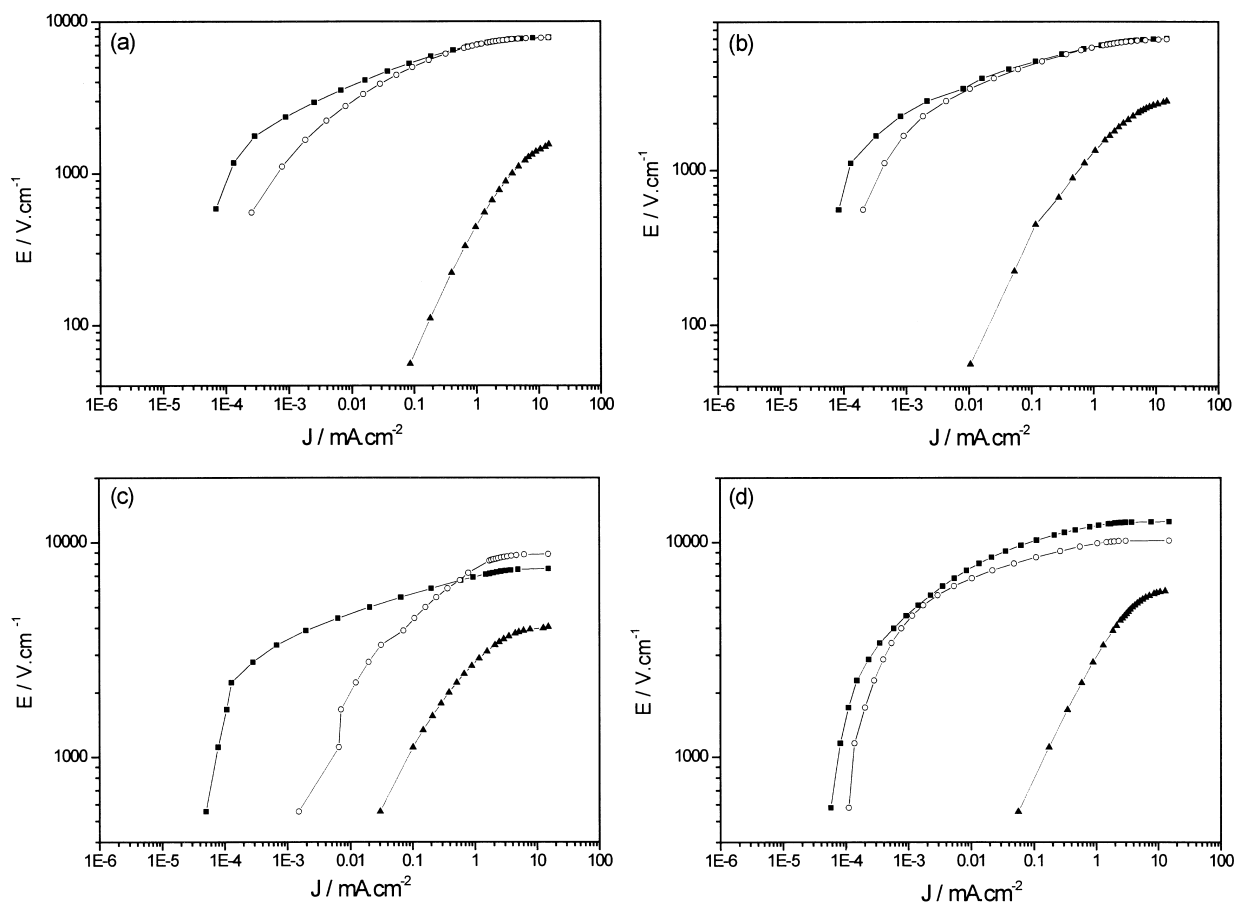


Fig. 4.  $I$ - $V$  characteristic curves (on a logarithmic scale) of SCNLa systems: (a) 0.05 mol% of La<sub>2</sub>O<sub>3</sub>; (b) 0.10 mol% of La<sub>2</sub>O<sub>3</sub>; (c) 0.15 mol% of La<sub>2</sub>O<sub>3</sub>; (d) 0.30 mol% of La<sub>2</sub>O<sub>3</sub>: (■) 1250°C at a cooling rate of 10°C min<sup>-1</sup>; (●) 1250°C at a cooling rate of 5°C min<sup>-1</sup>; (□) 1250°C at a cooling rate of 2°C min<sup>-1</sup>; (○) 1300°C at a cooling rate of 2°C min<sup>-1</sup>.

The X-ray diffraction pattern shows only one phase for the  $\text{SnO}_2\text{-CoO}$ -based varistor systems, in which CoO forms a solid solution through the substitution of  $\text{Sn}^{+4}$  ions for  $\text{Co}^{+2}$  or  $\text{Co}^{+3}$  ions, as discussed in earlier reports.<sup>1,3,8</sup> A  $\text{Co}_2\text{SnO}_4$  precipitated phase at the grain boundary is determined only when the EDS stage attached to the high resolution TEM and electron diffraction is used.<sup>8</sup> The absence of experimental evidence for eutectic liquid suggests that the densification observed in this system is not associated with liquid-phase sintering and that the sintering of the  $\text{SnO}_2\text{-CoO}$ -based system is controlled by solid-state diffusion. Therefore, the defects resulting from the presence of CoO in the grain boundary region of this polycrystalline ceramic material can contribute to potential barrier formation insofar as they are present in different valence states at the grain boundary interface, just as  $\text{Cr}_2\text{O}_3$  is, rendering this interfacial region richer in oxygen than the bulk region. The contribution of  $\text{Cr}_2\text{O}_3$  to the  $\alpha$  and  $E_b$  values has been described in earlier reports.<sup>1,9–11</sup>

The results obtained in this work suggest that  $\text{La}_2\text{O}_3$  also affects the grain boundary properties of  $\text{SnO}_2$  non-ohmic ceramics. Similarly to the Co element, therefore, the La element may present several valence states. Thus, if it can also be preferentially present in the grain

boundary region, like Co and Cr atoms, it may also cause effects similar to those promoted by CoO and  $\text{Cr}_2\text{O}_3$ <sup>1,9–11</sup> dopants, increasing the oxygen species (which can trap electrons) at the grain boundary interface, altering the trapping state density and the potential barrier feature.

The dopants used in the traditional ZnO-based varistor system play three major roles in forming the varistor. They can affect grain growth, the wetting characteristics of the liquid phase during cooling, and the electronic defect states that control the overall varistor characteristics. In the  $\text{SnO}_2\text{-CoO}$ -based varistor, the dopants may initially control only grain growth and electronic defect states due to this varistor's apparently single phase microstructure. However, a slight change in the chemistry of the precipitates and of metal segregation or secondary phase grain boundary (only visible by TEM microanalysis) can alter the density of states in this region of the material, changing its non-ohmic electrical behavior. Therefore, the results presented here reveal that the nonlinear properties of  $\text{SnO}_2$ -based varistors are more sensitive to small concentrations of dopants than the nonlinear properties of ZnO-based varistors, suggesting that these properties affect the electronic defect states, particularly, the defects existing near the grain boundary region, which are responsible for the

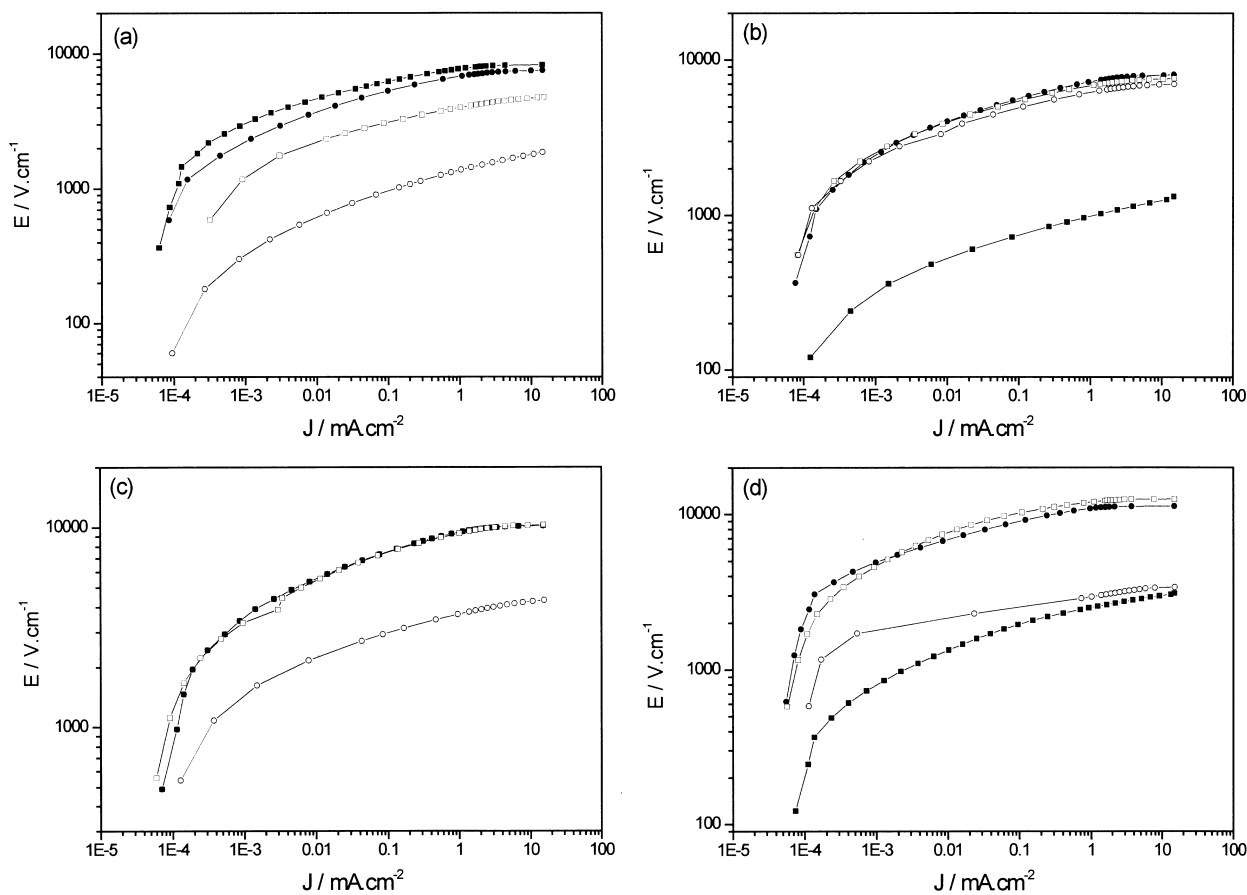


Fig. 5.  $I$ - $V$  characteristic curves (on a logarithmic scale) of SCNLa systems sintered at  $1250^\circ\text{C}$  using a cooling rate of  $2^\circ\text{C min}^{-1}$ : (a) 0.05 mol% of  $\text{La}_2\text{O}_3$ ; (b) 0.10 mol% of  $\text{La}_2\text{O}_3$ ; (c) 0.15 mol% of  $\text{La}_2\text{O}_3$ ; (d) 0.30 mol% of  $\text{La}_2\text{O}_3$ : (■) normal atmosphere; (○)  $\text{O}_2$ -rich atmosphere; (▲)  $\text{N}_2$ -rich atmosphere.

Table 4

Influence of 30 min atmosphere treatment at 900°C on  $\alpha$  and  $E_b$  values. SCNLa 0.05 mol% of  $\text{La}_2\text{O}_3$  sintered at 1250°C with a cooling rate of 2°C min<sup>-1</sup>

La <sub>2</sub> O <sub>3</sub> mol%	N <sub>2</sub> -rich atmosphere			O <sub>2</sub> -rich atmosphere		
	$\alpha$	$E_b/\text{V cm}^{-1}$	$\nu_b$ (V/barrier)	$\alpha$	$E_b/\text{V cm}^{-1}$	$\nu_b$ (V/barrier)
0.05	2	457	0.1	18	7172	1.8
0.10	4	1277	0.3	20	6158	1.4
0.15	6	2751	0.5	18	7959	1.6
0.30	5	3009	0.5	43	9636	1.5

potential barrier characteristics. This is an additional argument supporting the hypothesis that the La doped element is segregated near the grain boundary region, as was previously assumed when we discussed the effect of  $\text{La}_2\text{O}_3$  on the porosity of the studied samples.

Still on the same subject, it is easy to understand how the atmosphere treatment influences the nonlinear features of these new polycrystalline materials. The influence exerted by atmosphere treatment at 900°C on the  $\alpha$  and  $E_b$  values is significant, as can be seen in Table 4. This table shows  $\alpha$ ,  $E_b$  and  $\nu_b$  values for the SCNLa systems sintered at 1250°C, with a cooling rate of 2°C min<sup>-1</sup>, after treatment in an N<sub>2</sub>-rich atmosphere and a second thermal treatment in an O<sub>2</sub>-rich atmosphere. The N<sub>2</sub>-rich atmosphere treatment decreases the  $\alpha$ ,  $E_b$  and  $\nu_b$  values of these systems. However, this effect is reversible, because after the second thermal treatment in an O<sub>2</sub>-rich atmosphere,  $\alpha$ ,  $E_b$  and  $\nu_b$  values are restored close to their original values.

The reversible behavior of non-ohmic properties with atmosphere treatment, which has already been discussed in the literature,<sup>5–7,11</sup> is related to the potential barrier formation and to O<sub>2</sub> species at the grain boundary that cause trapping states and a Schottky-like barrier. This reversibility is assumed to be associated with the degree of oxidation (when the material is treated in an O<sub>2</sub>-rich atmosphere) or of reduction (when the material is treated in an N<sub>2</sub>-rich atmosphere) of metal oxides precipitated at the grain boundary. Thus, the role of  $\text{La}_2\text{O}_3$  is to provide the grain region with oxygen and increase the nonlinearity of the varistor system, since the barrier characteristics can be affected by oxygen species at the grain boundary as a consequence of this chemical change in the grain boundary region.

It is important to point out here that similar results for varistors that have been heated in reducing and oxidizing-rich atmospheres have already been reported by Sonder et al.<sup>12</sup> for the traditional ZnO-based varistor. The measurement of the  $I$ - $V$  characteristics of the ZnO-based varistor is the same as that presented in Fig. 5, which reveals that treatment in reducing atmospheres increases the leakage current, destroying the varistor characteristics, an effect that, as in the case of the SnO<sub>2</sub>-based varistor, can be reversed by annealing in oxygen.

The variation of the  $\nu_b$  values (in Table 4) with the thermal treatments in O<sub>2</sub>- and N<sub>2</sub>-rich atmospheres at 900°C is evidence that a preferential change in the grain boundary region occurs in the material. This variation reinforces the arguments presented earlier herein and the proposed mechanism [Eqs. (1)–(3)] to explain the influence of processing and small concentrations of dopants on the non-ohmic properties of SnO<sub>2</sub>-CoO-based varistor systems.

#### 4. Conclusions

The sensitivity of SnO<sub>2</sub>-CoO-based varistor properties to small concentrations of  $\text{La}_2\text{O}_3$  is similar to that previously reported for Cr<sub>2</sub>O<sub>3</sub>. Similarly to Cr<sub>2</sub>O<sub>3</sub>,  $\text{La}_2\text{O}_3$  is apparently present in the grain boundary region and may alter the potential barrier at the grain boundary, affecting the varistor properties. Moreover, the concentration of  $\text{La}_2\text{O}_3$ , sintering temperature and cooling rate also alter the properties of SnO<sub>2</sub>-CoO-based varistor properties. The best nonlinear property in this study was obtained using a cooling rate of 2°C min<sup>-1</sup>.

Thermal post-treatment in an N<sub>2</sub>-rich atmosphere decreases the nonlinear properties of samples. However, repeating the thermal treatment in O<sub>2</sub>-rich atmospheres can recover the nonlinear properties to nearly their original values. The sensitivity of SnO<sub>2</sub>-CoO non-ohmic properties to processing and to small concentrations of  $\text{La}_2\text{O}_3$  dopant was attributed to the degree of oxidation in the grain boundary region.

#### Acknowledgements

The financial support for this research work by the Brazilian research funding agencies FINEP/PRONEX, CNPq and FAPESP is gratefully acknowledged.

#### References

1. Jarzebski, Z. M. and Marton, J. P., Physical properties of SnO<sub>2</sub> materials — Part I. Preparation and defect structure. *J. Electrochem. Soc.*, 1976, **123**, 199C–205C.

2. Pianaro, S. A., Bueno, P. R., Longo, E. and Varela, J. A., A new SnO<sub>2</sub>-based varistor system. *J. Mater. Sci. Lett.*, 1995, **14**, 692–694.
3. Cerri, J. A., Leite, E. R., Gouvea, D. and Longo, E., Effect of cobalt (II) oxide and manganese (IV) oxide on sintering of tin (IV) oxide. *J. Am. Ceram. Soc.*, 1996, **79**, 799–804.
4. Pizarro, A. R., *Influência de dopantes na degradação do varistor a base de SnO<sub>2</sub>*. PhD thesis, Federal University of São Carlos, Brazil, 1997.
5. Bueno, P. R., Cassia-Santos, M. R., Leite, E. R., Longo, E., Bisquert, J., Garcia-Belmonte, G. and Fabregat-Santiago, F., Nature of the Schottky-type barrier of highly dense SnO<sub>2</sub> systems displaying non-ohmic behavior. *J. Appl. Phys.*, 2000, **88**, 6545–6548.
6. Cassia-Santos, M. R., Bueno, P. R., Longo, E. and Varela, J. A., Effect of oxidizing and reducing atmospheres on the electrical properties of dense SnO<sub>2</sub>-based varistor. *J. Eur. Ceram. Soc.*, in press.
7. Leite, E. R., Nascimento, A. M., Bueno, P. R., Longo, E. and Varela, J. A., The influence of sintering process and atmosphere on the non-ohmic properties of SnO<sub>2</sub> based varistor. *J. Mater. Sci.*, 1999, **10**, 321–327.
8. Varela, J. A., Cerri, J. A., Leite, E. R., Longo, E., Shamsuzzoha, M. and Bradt, R. C., Microstructural evolution during sintering of CoO doped SnO<sub>2</sub> ceramics. *Ceramics International*, 1999, **25**, 253–256.
9. Pianaro, S. A., Bueno, P. R., Olivi, P., Longo, E., Varela, J. A. Electrical properties of the SnO<sub>2</sub>-based varistor. *J. Mater. Sci. Electr.*, 1998, **9**, 159–165.
10. Bueno, P. R., Pianaro, S. A., Pereira, E. C., Bulhões, L. O. S., Longo, E. and Varela, J. A., Investigation of the electrical properties of SnO<sub>2</sub> varistor system using impedance spectroscopy. *J. Appl. Phys.*, 1998, **84**, 3700–3705.
11. Pianaro, S. A., Bueno, P. R., Longo, E. and Varela, J. A., Microstructure and electric properties of a SnO<sub>2</sub>-based varistor. *Ceramics International*, 1999, **25**(11), 1–6.
12. Sonder, E., Austin, M. M. and Kinser, D. L., Effect of oxidizing and reducing at atmospheres at elevated temperatures on the electrical properties of zinc oxide varistors. *J. Appl. Phys.*, 1983, **54**(6), 3566–3571.